Alkyne-Alkenyl Coupling at a Diruthenium Complex

Giulio Bresciani,[a] Serena Boni,[a] Stefano Zacchini,[b] Guido Pampaloni,[a] Marco Bortoluzzi,[c,*] Fabio Marchetti [a,*]

[a] University of Pisa, Department of Chemistry and Industrial Chemistry, Via G. Moruzzi 13, I-56124 Pisa, Italy.

[b] University of Bologna, Department of Industrial Chemistry "Toso Montanari", Viale Risorgimento 4, I-40136 Bologna, Italy.

[c] University of Venezia "Ca' Foscari", Department of Molecular Science and Nanosystems, Via Torino 155, I-30170 Mestre (VE), Italy.

Corresponding Authors

*E-mail addresses: markos@unive.it; fabio.marchetti1974@unipi.it

Webpage: https://people.unipi.it/fabio_marchetti1974/

ORCID-ID:

Giulio Bresciani: 0000-0003-4239-8195

Stefano Zacchini: 0000-0003-0739-0518

Guido Pampaloni: 0000-0002-6375-4411

Marco Bortoluzzi: 0000-0002-4259-1027

Fabio Marchetti: 0000-0002-3683-8708

Abstract

Dimetallic complexes are suitable platforms for the assembly of small molecular units, and the reactivity of bridging alkenyl ligands has been widely investigated to model C-C bond forming processes. Here, we report the unusual coupling of an alkenyl ligand, bridging coordinated on a diruthenium scaffold, with a series of alkynes, revealing two possible outcomes. The diruthenium complex $[Ru_2Cp_2(Cl)(CO)(\mu\text{-}CO)\{\mu\text{-}\eta^1\text{:}\eta^2\text{-}C(Ph)=CH(Ph)\}]$, **2**, was prepared in two steps from $[Ru_2Cp_2(CO)_2(\mu\text{-}CO)\{\mu\text{-}\eta^1\text{:}\eta^2\text{-}C(Ph)=CH(Ph)\}]BF_4$, **[1]BF$_4$**, in 69% yield. Then, the reaction of **2** with $C_2(CO_2Me)_2$, promoted by $AgCF_3SO_3$ in dichloromethane, afforded in 51% yield the complex $[Ru_2Cp_2(CO)_2\{\mu\text{-}\eta^3\text{:}\eta^2\text{-}C(Ph)CH(Ph)C(CO_2Me)C(CO_2Me)\}]CF_3SO_3$, [**3**]$CF_3SO_3$, containing a ruthenacyclopentene-based hydrocarbyl ligand. On the other hand, **2** reacted with other alkynes and AgX salts to give the butadienyl complexes $[Ru_2Cp_2(CO)_2\{\mu\text{-}\eta^3\text{:}\eta^2\text{-}C(R)CH(R')C(Ph)C(Ph)\}]X$ (R = R′ = H, [**4**]BF_4; R = R′ = Me, [**5**]CF_3SO_3; R = R′ = Ph, [**6**]CF_3SO_3; R = Ph, R′ = H, [**7**]CF_3SO_3), in 42-56% yields. All products were characterized by IR and NMR spectroscopy, and by single crystal X-ray diffraction in the cases of **2**, [**3**]CF_3SO_3 and [**6**]BF_4. DFT calculations highlighted the higher stability of [**4-7**]$^+$-like structures with respect to the corresponding [**3**]$^+$-like isomers. It is presumable that [**3**]$^+$-like isomers initially form as kinetic intermediates, then undergoing H-migration which is disfavoured in the presence of carboxylato substituents on the alkyne. Such hypothesis was supported by the computational optimization of the transition states for H-migration in the cases of R = R′ = H and R = R′ = CO_2Me.

Keywords: organometallic synthesis; diruthenium complexes; μ-alkenyl ligand; C-C bond formation; alkyne insertion.

Introduction

Dimetallic complexes, exploiting cooperative effects supplied by the two metal centres in close proximity, represent ideal scaffolds to study a multitude of reaction pathways otherwise hardly

available on related mononuclear complexes.[1,2,3] For instance, as two working hands compared to one single hand, dimetallic systems offer major opportunities to build and stabilize uncommon hydrocarbyl ligands via multisite bridging coordination.[4,5,6,7,8,9,10] Alkynes are useful and versatile reagents in this setting, and in particular the $\{M_2Cp_2(CO)_x\}$ scaffold (M = Fe, Ru; Cp = η^5-C_5H_5; x = 2, 3) is suitable to promote their coupling with a diversity of bridging coordinated carbon ligands, including carbonyl,[11,12] isocyanide,[13] thiocarbonyl,[14] alkylidyne[10,15,16] and alkylidene ligands,[17,18,19,20] usually via alkyne insertion into the metal-μ-carbon bond, but alternative modes are also possible.[21] The two metal coordination spheres are coordinatively and electronically saturated, therefore prior removal of one 2-electron ligand (usually, a carbon monoxide ligand) is needed to guarantee the initial η^2-coordination of the alkyne to one metal centre, that is a preliminary, fundamental step along the coupling process.[22] The CO displacement is preferentially performed by substitution with the labile acetonitrile ligand using the trimethylamine-N-oxide (TMNO) strategy, which is often reliable on cationic complexes;[15,23,24,25,26] when this strategy is not applicable, photolytic methods can be employed, although they might be featured by a low degree of selectivity.[13,14,19]

Dimetallic complexes with a bridging alkenyl (vinyl) ligand, {-C(R)=C(R′)(R′′)}, have been widely investigated as simplified models for C-C coupling events, with a particular focus on the elucidation of the mechanism of the Fischer-Tropsch reaction (FT), wherein alkenyl units are involved in the growing of the linear hydrocarbon chain.[9,27,28,29,30] To the best of our knowledge, the coupling reaction between simple alkenyl ligands and external alkynes has been unexplored heretofore. On the other hand, the coupling of alkynes with alkenyl molecules is of ultimate relevance in metal-mediated organic synthesis,[31,32,33,34,35,36] and the alkyne insertion into metal-alkenyl bonds constitutes a key step of the important Dötz reaction.[37,38,39]

We selected the diruthenium complex $[Ru_2Cp_2(CO)_2(\mu\text{-}CO)\{\mu\text{-}\eta^1\text{:}\eta^2\text{-}C(Ph)=CH(Ph)\}]BF_4$, **[1]BF$_4$**, as a convenient starting material to provide a chance for the μ-alkenyl-alkyne coupling; Knox and co-workers previously demonstrated that complexes homologous to **[1]BF$_4$**, bearing different alkenyl

substituents, display a versatile chemistry.[40] Compound **[1]BF4** was prepared by HBF_4 protonation of the dimetallacyclopentenone precursor $[Ru_2Cp_2(CO)(\mu\text{-}CO)\{\mu\text{-}\eta^1\text{:}\eta^3\text{-}C_2Ph_2C(O)\}]$,[41] for which we recently optimized the synthetic procedure from commercial $[Ru_2Cp_2(CO)_4]$, Scheme 1.[42]

The results of the present synthetic study highlight two possible outcomes for the alkenyl-alkyne coupling.

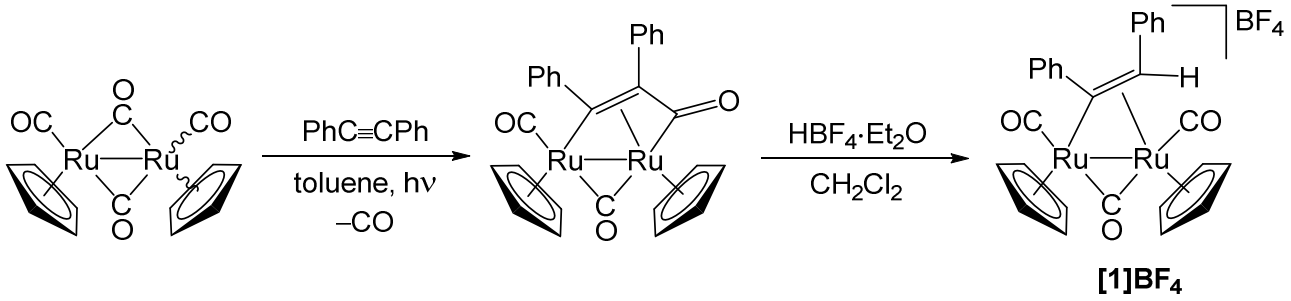

Scheme 1. Two-step synthesis of diruthenium complex with a $\mu\text{:}\eta^1\text{:}\eta^2$-(bis-phenyl)alkenyl ligand.

Results and discussion

Synthesis and characterization of complexes

To promote the reaction of **[1]BF4** with alkynes, first a dichloromethane solution of this complex was treated with TMNO in the presence of acetonitrile, to afford the acetonitrile adduct **[1-NCMe]BF4** (Scheme 2); the formation of **[1-NCMe]BF4** was easily checked via solution IR spectroscopy (see Experimental for details). The subsequent reactions of freshly prepared **[1-NCMe]BF4** with a series of alkynes resulted in the formation of complicated mixtures of products. Therefore, **[1-NCMe]BF4** was converted into the chloride derivative **2**, upon treatment with lithium chloride in THF (Scheme 2). In fact, the abstraction of a chloride ligand by means of a silver salt, in several cases, has proved to be a clean alternative to generate a coordination vacancy on group 8 metal centres, enabling the subsequent coordination of organic reactants.[10,15]

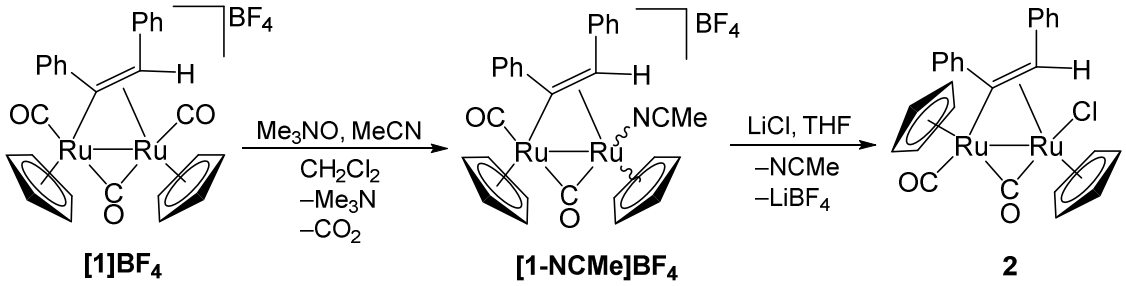

Scheme 2. Two-step carbonyl-chloride substitution on diruthenium μ-alkenyl complex.

The reaction leading to **2** was straightforward, and this product was isolated in 69% yield after chromatographic purification on alumina, and fully structurally characterized. The X-ray structure of **2** consists of a [*trans*-$Ru_2Cp_2(Cl)(CO)(\mu\text{-}CO)$] core bonded to a $\mu:\eta^1:\eta^2$-(bis-phenyl)alkenyl ligand. (Figure 1). It must be remarked that the closely related alkenyl complex $[Ru_2Cp_2(Cl)(CO)(\mu\text{-}CO)\{\mu\text{-}\eta^1:\eta^2\text{-}C(H)=CH(CO_2Et)\}]$ shows a *cis* arrangement of the Cp ligands.[43] Despite the different stereochemistry, the bonding parameters of **2** and $[Ru_2Cp_2(Cl)(CO)(\mu\text{-}CO)\{\mu\text{-}\eta^1:\eta^2\text{-}C(H)=CH(CO_2Et)\}]$ are similar. As usually observed for dinuclear $\mu\text{-}\eta^1:\eta^2$-alkenyl complexes, the Ru(1)-C(1) [2.0806(19) Å] and Ru(2)-C(1) [2.1700(18) Å] distances are comparable,[43] and the C(1)-C(2) contact [1.413(3) Å] is elongated compared to a C=C double bond [1.34 Å] due to the coordination to Ru(2).

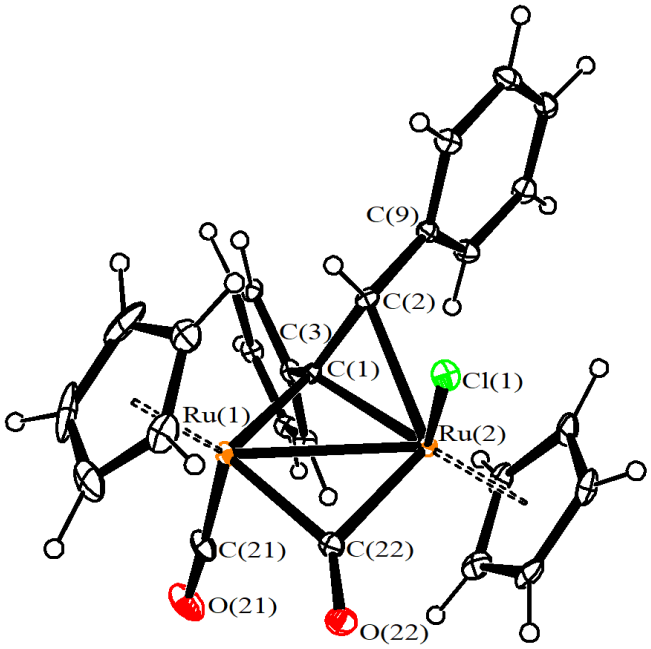

Figure 1. View of the molecular structure of **2**. Displacement ellipsoids are at the 30% probability level. Selected bond lengths (Å) and angles (°): Ru(1)-Ru(2) 2.7433(2), Ru(1)-Cp_{av} 2.256(4), Ru(2)-Cp_{av} 2.207(4), Ru(1)-C(21) 1.861(2), Ru(1)-C(22) 2.001(2), Ru(2)-C(22) 2.072(2), Ru(2)-Cl(1) 2.4345(5), Ru(1)-C(1) 2.0806(19), Ru(2)-C(1) 2.1700(18), Ru(2)-C(2) 2.2480(19), C(1)-C(2) 1.413(3), C(1)-C(3) 1.489(3), C(2)-C(9) 1.482(3), C(21)-O(21) 1.143(3), C(22)-O(22) 1.168(3), Ru(1)-C(21)-O(21) 175.3(2), Ru(1)-C(1)-Ru(2) 80.36(7), Ru(1)-C(22)-Ru(2) 84.65(8), Ru(1)-C(1)-C(2) 115.28(13), C(1)-C(2)-C(9) 127.01(17), C(1)-C(2)-Ru(2) 68.37(11).

The IR spectrum of **2** (in CH_2Cl_2) exhibits two absorptions related to the terminal and bridging carbonyls, respectively (1977 and 1828 cm^{-1}). The NMR spectra (in $CDCl_3$) consist of one set of resonances, suggesting that **2** exists in solution in the same *trans* configuration as observed in the solid state; since **[1]BF$_4$** was previously ascertained to exist as a *cis* isomer,[12] the carbonyl-chloride substitution is accompanied by a *cis* to *trans* rearrangement of the {Ru_2Cp_2} core. In the ^{13}C spectrum, the alkenyl carbons resonate at 155.1 (Ru-C) and 83.7 ppm (=CH); in particular, the downfield resonance exhibited by the ruthenium-bound carbon indicates some bridging alkylidene character,[8,44,45] in alignment with the X-ray evidence that such carbon is nearly equidistant between the two ruthenium atoms.

The reactivity of **2** with a series of alkynes was investigated in dichloromethane solution using, in each case, an excess of the alkyne and silver triflate or silver tetrafluoroborate as chloride abstractor, Scheme 3.

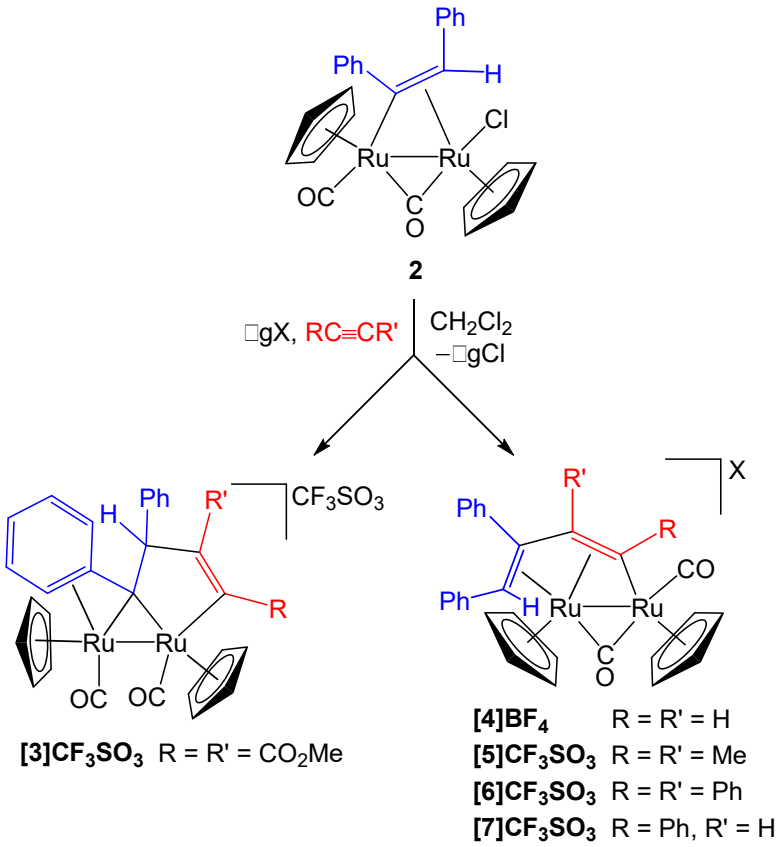

Scheme 3. □lkenyl-alkyne coupling on a diruthenium scaffold.

Thus, the reaction of **2** with dimethyl acetylenedicarboxylate and silver trifluoromethanesulfonate resulted in the selective formation of **[3]CF_3SO_3**, which was isolated in 51% yield after work-up. The structure of **[3]CF_3SO_3**·CH_2Cl_2 was ascertained by single crystal X-ray diffraction (Figure 2 and Table 1). The cation, [**3**]$^+$, is composed of the {*trans*-$Ru_2Cp_2(CO)_2$} core to which is coordinated the unprecedented {μ-η^2:η^3-C(Ph)-CH(Ph)-C(CO_2Me)=C(CO_2Me)} ligand. The latter is bonded to the Ru centres through four carbon atoms, i.e. a bridging alkylidene, a η^2-phenyl and a terminal σ-alkenyl fragment. Indeed, the Ru(1)-C(3) [2.083(5) Å] and Ru(2)-C(3) [2.153(5) Å] contacts are typical for a bridging alkylidene (carbene) ligand,[46,47,48,49] and the Ru(1)-C(6) distance [2.077(5) Å] is in keeping with a single bond involving a sp^2 carbon atom. The C(5)-C(6) contact [1.336(7) Å] is essentially a double bond, whereas C(3)-C(4) [1.538(6) Å] and C(4)-C(5) [1.509(7) Å] are almost pure single bonds. Overall, the Ru(1)-C(3)-C(4)-C(5)-C(6) ring may be described as a ruthenacyclopentene comprising a bridging alkylidene carbon, whose bonding parameters are comparable to those reported

in the literature for the unique example of analogous ruthenacycle.[50] The ruthenacyclopentene ring is almost planar [mean deviation from the least square plane 0.037 Å] and both C(5) and C(6) are hybridized sp^2 [sum angles 360.0(8)° and 359.8(6)°, respectively]. The Ru(2)-C(17) [2.272(5) Å] and Ru(2)-C(22) [2.446(5) Å] distances are in the range reported for Ru bonded to a η^2-phenyl ligand.[51,52,53] Coordination to Ru(2) via a single C-C edge results in a reduced delocalization within the phenyl ring, as indicated by the presence of alternated longer and shorter bonds, that is C(17)-C(18) [1.443(7) Å], C(18)-C(19) [1.361(7) Å], C(19)-C(20) [1.413(7) Å], C(20)-C(21) [1.354(7) Å], C(21)-C(22) [1.424(7) Å] and C(17)-C(22) [1.411(7) Å].

The Ru(1)-C(1) contact [1.880(5) Å] is significantly shorter than Ru(2)-C(2) [1.925(5) Å], pointing out a greater π-back donation from Ru(1) to the terminal CO ligand compared to Ru(2). This is in keeping with the localization of the positive charge on Ru(2), which would formally reach 19 valence electrons in the absence of the positive charge. It must be remarked that both Ru(1)···C(2) [3.129(6) Å] and Ru(2)···C(1) [2.872(6) Å] are essentially non-bonding, in full accordance with terminal coordination of the carbonyls.

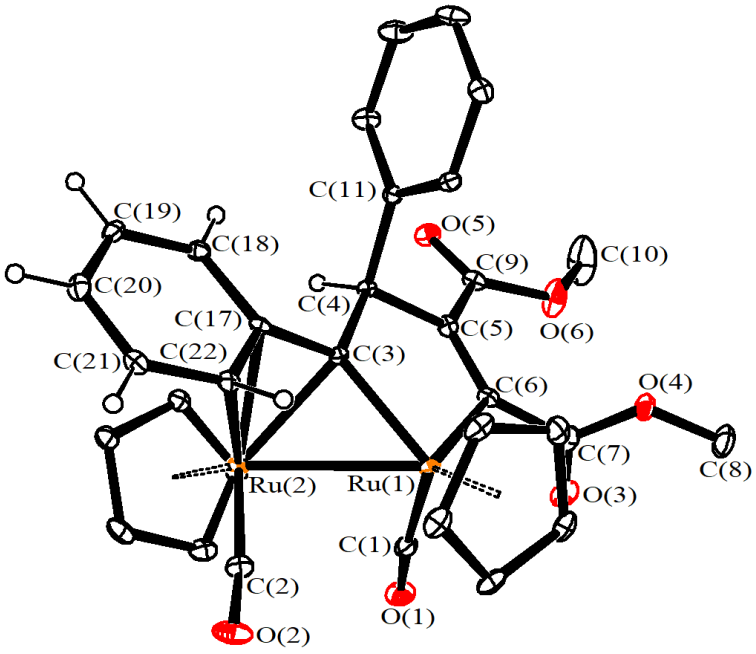

Figure 2. View of the molecular structure of [**3**]⁺. Displacement ellipsoids are at the 30% probability level. H-atoms, except H(4) and H(18)-H(22), have been omitted for clarity.

Table 1. Selected bond lengths (Å) and angles (°) for **[3]**$^{+}$

Ru(1)-Ru(2)	2.8041(6)	Ru(1)-C(1)	1.880(5)
Ru(2)-C(2)	1.925(5)	Ru(1)-C(3)	2.083(5)
Ru(2)-C(3)	2.153(5)	Ru(2)-C(17)	2.272(5)
Ru(2)-C(22)	2.446(5)	Ru(1)-C(6)	2.077(5)
Ru(1)-Cp_{av}	2.253(11)	Ru(2)-Cp_{av},	2.206(11)
C(3)-C(4)	1.538(6)	C(4)-C(5)	1.509(7)
C(5)-C(6)	1.336(7)	C(6)-C(7)	1.493(7)
C(3)-C(17)	1.457(7)	C(4)-C(11)	1.522(6)
C(5)-C(9)	1.482(7)	C(17)-C(18)	1.443(7)
C(18)-C(19)	1.361(7)	C(19)-C(20)	1.413(7)
C(20)-C(21)	1.354(7)	C(21)-C(22)	1.424(7)
C(17)-C(22)	1.411(7)	C(9)-O(5)	1.208(6)
C(9)-O(6)	1.337(7)	C(7)-O(3)	1.194(7)
C(7)-O(4)	1.339(7)	C(1)-O(1)	1.139(6)
C(2)-O(2)	1.127(6)		
Ru(1)-C(1)-O(1)	174.1(5)	Ru(2)-C(2)-O(2)	173.7(5)
Ru(1)-C(3)-Ru(2)	82.87(17)	C(3)-C(4)-C(5)	108.0(4)
C(4)-C(5)-C(6)	117.3(4)	C(4)-C(5)-C(9)	116.4(4)
C(6)-C(5)-C(9)	126.3(5)	C(5)-C(6)-C(7)	123.2(4)
C(5)-C(6)-Ru(1)	119.5(4)	C(7)-C(6)-Ru(1)	117.1(3)
C(3)-C(17)-C(22)	120.6(4)	C(3)-C(17)-C(18)	122.1(4)
C(18)-C(17)-C(22)	116.2(4)	C(17)-C(18)-C(19)	121.2(5)
C(18)-C(19)-C(20)	121.1(5)	C(19)-C(20)-C(21)	119.9(5)
C(20)-C(21)-C(22)	120.2(5)	C(21)-C(22)-C(17)	121.4(4)
Sum at C(7)	359.8(8)	Sum at C(9)	359.9(8)

In the IR spectrum of **[3]CF_3SO_3** in dichloromethane solution, two absorptions were detected at 2026 and 2002 cm^{-1}, in accordance with the terminal coordination fashion adopted by the two carbonyl ligands in the solid state; moreover, a strong infrared band at 1712 cm^{-1} accounts for the ester groups originally belonging to the alkyne. The NMR spectra (in acetone-d_6 solution) display one set of resonances. In the ^1H spectrum, the signals related to the phenyl moieties fall in the range 8.32-7.74 ppm, including the proton bound to the carbon involved in metal coordination; in a variety of dinuclear compounds comprising a μ-η^1:η^3-phenyl-alkylidene, such proton has been reported to resonate in a wide range (7.3 - 1.1 ppm) of chemical shifts.[54,55,56,57,58,59,60]

Salient ^{13}C signals are those related to the terminal carbonyl ligands (216.2 and 203.0 ppm), the bridging alkylidene carbon (174.8 ppm) and the other members of the metallacyclopentene ring, which were found at 74.2 (CHPh), 105.0 and 126.2 ppm (C=C).

The formation of **[3]**$^+$ presumably proceeds with initial η^2-coordination of the alkyne to the ruthenium,[22] once the chloride ligand in **2** has been displaced by Ag^+, followed by C-C bond coupling between the alkyne and the distal alkenyl carbon.

Surprisingly, the reactions of **2** with other alkynes, in the presence of a silver salt, did not lead to products analogous to **[3]**$^+$. As a matter of fact, ethyne, 2-butyne, diphenylacetylene and phenylacetylene were involved in an apparent insertion into the ruthenium-alkenyl bond to afford the diruthenium μ-butadienyl cations [**4-7**]$^+$. In order to collect X-ray quality crystals, the synthesis of [**6**]$^+$ was repeated using $AgBF_4$ as silver salt (see Supporting Information for details), then the structure of **[6]BF$_4$** was determined by single crystal X-ray diffraction (Figure 3 and Table 2). The cation [**6**]$^+$ consists of the {*cis*-$Ru_2Cp_2(CO)(\mu\text{-}CO)$} core bonded to the {μ-$\eta^1$:$\eta^4$-C(Ph)=C(Ph)-C(Ph)=CH(Ph)} butadienyl ligand. In agreement with this, the C(3)-C(4) [1.427(4) Å] and C(5)-C(6) [1.421(4) Å] bonds are shorter than C(4)-C(5) [1.457(4) Å]. The present example represents the first case of structurally characterized diruthenium bis-cyclopentadienyl complex with a butadienyl ligand coordinated through the μ-η^1:η^4-fashion. Knox and co-workers reported analogous μ-η^2:η^3-butadienyl compounds, obtained by the coupling of bridging methylene ligand with propargyl alcohols and subsequent H_2O elimination.[61]

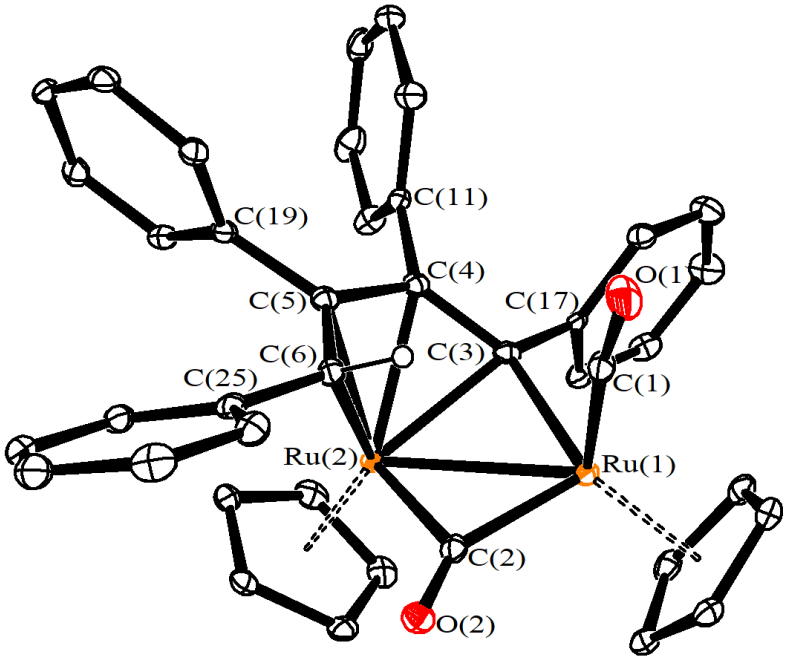

Figure 3. View of the molecular structure of [**6**]$^+$. Displacement ellipsoids are at the 30% probability level. H-atoms, except H(6), have been omitted for clarity.

Table 2. Selected bond lengths (Å) and angles (°) for [**6**]$^+$

Ru(1)-Ru(2)	2.7698(3)	Ru(1)-C(1)	1.882(3)
Ru(1)-C(2)	1.969(3)	Ru(2)-C(2)	2.200(3)
Ru(1)-C(3)	2.102(3)	Ru(2)-C(3)	2.163(3)
Ru(2)-C(4)	2.261(3)	Ru(2)-C(5)	2.227(3)
Ru(2)-C(6)	2.268(3)	Ru(1)-Cp_{av}	2.262(7)
Ru(2)-Cp_{av}	2.220(7)	C(1)-O(1)	1.136(4)
C(2)-O(2)	1.159(4)	C(3)-C(4)	1.427(4)
C(4)-C(5)	1.457(4)	C(5)-C(6)	1.421(4)
C(3)-C(17)	1.490(4)	C(4)-C(11)	1.511(4)
C(5)-C(19)	1.500(4)	C(6)-C(25)	1.483(4)
Ru(1)-C(1)-O(1)	172.7(3)	Ru(1)-C(2)-Ru(2)	83.06(12)
Ru(1)-C(3)-Ru(2)	80.97(10)	Ru(1)-C(3)-C(4)	135.1(2)
C(3)-C(4)-C(5)	125.5(3)	C(4)-C(5)-C(6)	121.3(3)
C(5)-C(6)-C(25)	125.2(3)		

The IR and NMR data obtained for the [**4-7**]$^+$ salts agree with the X-ray data collected for [**6**]$^+$. The IR spectra, in dichloromethane, clearly evidence the presence of one terminal (2006-2008 cm^{-1}) and one bridging carbonyl (1859-1884 cm^{-1}) ligands. The NMR spectra show two sets of resonances,

which have been assigned to *cis* and *trans* isomers (with reference to the mutual orientation of the Cp ligands). This attribution relies on DFT calculations, pointing out the comparable stability of *cis*- and *trans*-structures (vide infra), and is based on a comparison with the NMR data available for other $\{Ru_2Cp_2(CO)_2\}$ cationic derivatives containing strictly related bridging hydrocarbyl ligands.[41,42,61] For instance, in **[4]BF$_4$** the Cp ligands give rise to four ^{1}H resonances at 6.22 and 5.48 ppm (*cis*) and 5.68 and 5.59 ppm (*trans*). The *cis* isomer is the prevalent one in solution for [**4**]$^+$ and [**6**]$^+$, while the trans isomer prevails in [**5**]$^+$ and is the only one recognized for [**7**]$^+$. The bridging carbon, belonging to the butadienyl ligand and bound to both ruthenium centres, resonates in the range 165.2 – 192.6 ppm, reflecting its alkylidene nature. Accordingly, in the ^{1}H NMR spectrum of **[4]BF$_4$**, the {μ-CH} has been recognized in the typical downfield region (11.61 and 10.86 ppm for the *cis* and *trans* isomers, respectively).[12,62] The signals of the other carbon nuclei, going along the C_4 chain, fall in the intervals 99.1 – 111.9 ppm, 106.9 – 121.0 ppm and 74.4 – 87.8 ppm, respectively.

The reaction leading to **[7]CF$_3$SO$_3$** involves an unsymmetrical (terminal) alkyne, and takes place in a regiospecific manner, placing the alkyne substituent far from the alkenyl moiety; the ^{1}H NMR spectrum of the alternative isomer would display a downfield resonance (compare with [**4**]BF_4, see above) which has not been detected. The synthesis of **[7]CF$_3$SO$_3$** is accompanied by the formation of an unidentified, inseparable by-product (ca. 15% of the total), displaying Cp signals at 4.85 and 4.61 ppm.

DFT calculations

With the aim of elucidating the different outcomes of the coupling between the alkenyl ligand in **2** and alkynes, we carried out a DFT investigation focusing the attention on the potential isomers of **[3]**$^+$, **[4]**$^+$ and **[6]**$^+$. Ruthenacycle structures such as that described for **[3]CF$_3$SO$_3$**, indicated with **[3^a]**$^+$, **[4^a]**$^+$ and **[6^a]**$^+$, were considered together with the corresponding butadienyl derivatives analogous to **[6]BF$_4$** and indicated with **[3^b]**$^+$, **[4^b]**$^+$ and **[6^b]**$^+$. *Cis* and *trans* isomers were evaluated for all the structures. The superimposition of experimental (X-ray) and computed structures (PBEh-3c method)

for $[\mathbf{3^a_{trans}}]^+$ and $[\mathbf{6^b_{cis}}]^+$, respectively, is overall acceptable, with RMSD respectively of 0.222 and 0.294 Å. The RMSD values are 0.269 Å for $[\mathbf{3^a_{trans}}]^+$ and 0.269 Å for $[\mathbf{6^b_{cis}}]^+$ including the C-PCM solvation model (CH_2Cl_2 as continuous medium).

The relative Gibbs free energy values are summarized in Table 3 and plotted in Figure S13 together with the DFT-optimized structures. Thus, $[\mathbf{3^a_{trans}}]^+$ is more stable than $[\mathbf{3^a_{cis}}]^+$ by 4.5 kcal mol^{-1} (C-PCM calculations; 7.3 kcal mol^{-1} in gas phase), according to the X-ray findings and the observation of a single set of signals in the NMR spectra (see above). The cations $[\mathbf{4^b}]^+$ and $[\mathbf{6^b}]^+$ are more stable in the cis configuration rather than the trans one, with Gibbs energy differences comprised between 1.0 and 3.1 kcal mol^{-1}. This result is in keeping with the X-ray structure of **[6]BF$_4$** and justifies the existence in solution of mixtures of *cis* and *trans* isomers for $[\mathbf{4\text{-}7}]^+$. An additional stereoisomer might be conceived for $[\mathbf{6^b_{cis}}]^+$, with inverted orientations of Ph and H bound to C(6) carbon atom; it was computationally investigated (Figure S14) but resulted thermodynamically unfavourable by 11.3 kcal mol^{-1} (C-PCM calculations; 10.3 kcal mol^{-1} in gas phase).

Table 3. Relative Gibbs energy values (kcal mol^{-1}) for the potential isomers of **[3]$^+$**, **[4]$^+$** and **[6]$^+$** calculated with the PBEh-3c method in gas phase and with the C-PCM solvation model (CH_2Cl_2).

	C-PCM	GAS
$[\mathbf{3^a_{cis}}]^+$	0	0
$[\mathbf{3^a_{trans}}]^+$	-4.5	-7.3
$[\mathbf{3^b_{cis}}]^+$	-23.8	-29.8
$[\mathbf{3^b_{trans}}]^+$	-25.0	-32.3
$[\mathbf{4^a_{cis}}]^+$	0	0
$[\mathbf{4^a_{trans}}]^+$	-6.0	-7.4
$[\mathbf{4^b_{cis}}]^+$	-38.2	-38.4
$[\mathbf{4^b_{trans}}]^+$	-35.1	-35.7
$[\mathbf{6^a_{cis}}]^+$	0	0
$[\mathbf{6^a_{trans}}]^+$	-5.4	-7.5
$[\mathbf{6^b_{cis}}]^+$	-27.2	-31.3
$[\mathbf{6^b_{trans}}]^+$	-25.8	-30.3

In every cases, DFT calculations point out the higher stability of the butadienyl structures $[\mathbf{3^b}]^+$, $[\mathbf{4^b}]^+$ and $[\mathbf{6^b}]^+$ with respect to the corresponding ruthenacycle isomers, with Gibbs energy differences in the 20 to 30 kcal mol^{-1} range. Computational outcomes therefore suggest that the alkyne insertion

process leading to μ-η^1:η^4-butadienyl complexes is strongly favoured from a thermodynamic point of view, and that the unique formation of [**3**]$^+$ from **2** and dimethyl acetylenedicarboxylate should be ascribed to kinetic reasons related to the peculiar properties of the alkyne CO_2Me substituents.

We hypothesize that, following preliminary η^2-coordination to the metal centre, the alkyne generally couples with the distal carbon of the alkenyl ligand, thus forming a ruthenacycle of type [**3**]$^+$. The stable butadienyl products, [**4-7**]$^+$, would be subsequently generated via hydrogen 1,2-migration, as sketched in Scheme 4. The overall result is the observed pseudo-insertion reaction of alkynes into the Ru-alkenyl σ-bond shown in Scheme 3 (synthesis of [**4-7**]$^+$).

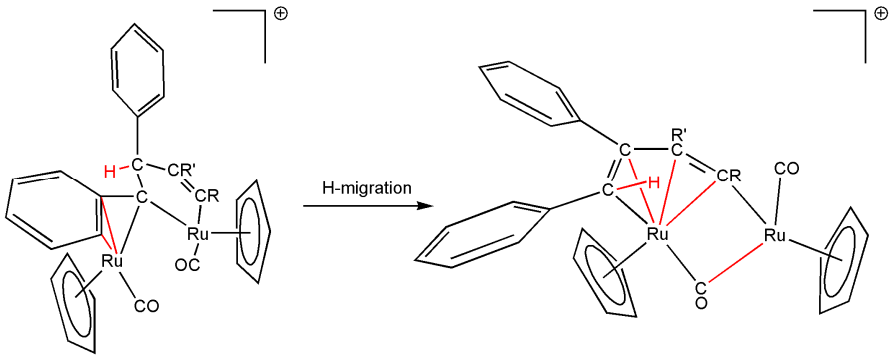

Scheme 4. Proposed formation of diruthenium butadienyl complexes (right) from H-migration in intermediate ruthenacycles (left).

The transition state associated with such presumably fundamental step was calculated at the DFT EDF2 level for the cations in *trans* configuration bearing R = R' = CO_2Me (**[3$^{TS}_{trans}$]**$^+$) and R = R' = H (**[4$^{TS}_{trans}$]**$^+$). In both cases, one imaginary frequency related to the proton shift was found, i885 cm^{-1} for **[3$^{TS}_{trans}$]**$^+$ and i836 cm^{-1} for **[4$^{TS}_{trans}$]**$^+$. The coherence of the localized transition states with the 1,2-proton shift was further confirmed by means of IRC calculations starting from **[4$^{TS}_{trans}$]**$^+$.[63] As depicted in Figure 4, the relative Gibbs energy of **[3$^{TS}_{trans}$]**$^+$ with respect to the **[3$^{a}_{trans}$]**$^+$ ground state geometry is 33.6 kcal mol^{-1}, meaningfully higher than the energy difference between **[4$^{TS}_{trans}$]**$^+$ and **[4$^{a}_{trans}$]**$^+$, that is 27.4 kcal mol^{-1}. It seems reasonable that the experimentally obtained product **[3]CF_3SO_3** is a kinetic one (**[3$^{a}_{trans}$]**$^+$), which is isolated thanks to the quite high energy barrier involved in its isomerization to the butadienyl derivative (**[3$^{b}_{trans}$]**$^+$, see Figure S13). Hence, we

assume that **[4-7]CF_3SO_3** are produced via the intermediate formation of kinetic species (not observed) analogous to **[3]CF_3SO_3**. We attempted to promote the conversion of **[3]CF_3SO_3** into its geometric isomer(s) analogous to **[4-7]$^+$** by heating a THF solution at reflux, but this thermal treatment activated decomposition pathways leading to mixtures of unidentified products. The divergent behaviour of dimethyl acetylenedicarboxylate, with respect to a series of different alkynes, was previously observed in the reactivity towards the heterodinuclear complex $[Fe(CO)_3(\mu\text{-dppm})(\mu\text{-CO})Pt(PPh_3)]$.[64]

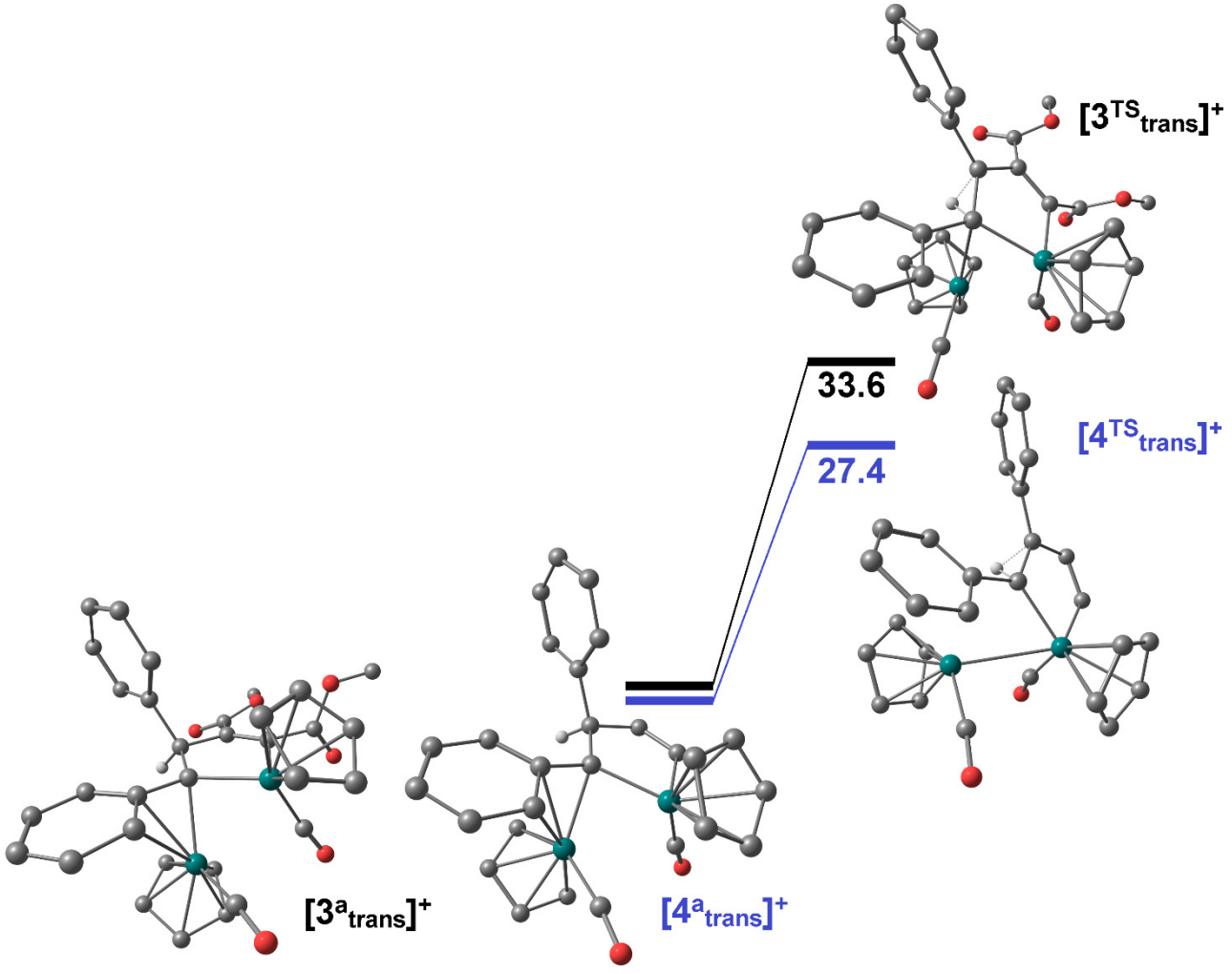

Figure 4. DFT-optimized structures of the cations **[3^a_{trans}]$^+$**, **[4^a_{trans}]$^+$**, **[3^{TS}_{trans}]$^+$** and **[4^{TS}_{trans}]$^+$**, and Gibbs energy barriers associated to the H-migration affording butadienyl ligands (kcal mol^{-1}, EDF2 calculations). Ru, green; O, red; C, white. Only the migrating hydrogen atom (white) is shown for clarity.

Conclusions

Dimetallic scaffolds offer much opportunity for the assembly of molecular units, exploiting the cooperative effects provided by two adjacent metal centres, and the coupling of bridging alkenyl ligands with a variety of small organic fragments was widely investigated in the past to gain insight into the mechanism of related solid-state reactions. In this setting, despite the relevance of the alkenyl-alkyne coupling in organic synthesis, the latter process was unexplored on di- or polymetallic frameworks. Here, we report a rare coupling event between a series of alkynes and an alkenyl ligand bridging coordinated on the $\{Ru_2Cp_2(CO)_2\}$ scaffold, involving the distal alkenyl carbon and confirming the versatility of such diruthenium framework to explore new modes of C-C bond formation. Two types of novel hydrocarbyl ligands stabilized by multisite coordination are selectively isolated, depending on the alkyne substituents. DFT calculations pointed out a plausible correlation between the two structures based on the 1,2-migration of a hydrogen atom, while alkyne insertion into Ru-C bond, otherwise frequently observed on similar systems, appears unlikely.

Experimental

Materials and methods. Reactants and solvents were purchased from Alfa Aesar, Merck, Strem or TCI Chemicals, and were of the highest purity available. Complex **[1]BF$_4$** was prepared according to the literature.[41,42] Reactions were conducted under dinitrogen atmosphere using standard Schlenk techniques. Products were stored in air once isolated. Dichloromethane and tetrahydrofuran were dried with the solvent purification system mBraun MB SPS5, while acetonitrile was distilled from CaH_2. IR spectra of solutions were recorded using a CaF_2 liquid transmission cell (2300-1500 cm^{-1}) on a Perkin Elmer Spectrum 100 FT-IR spectrometer. IR spectra were processed with Spectragryph software.[65] ^1H and ^{13}C spectra were recorded at 298 K on a Jeol JNM-ECZ400S instrument equipped with a Royal Broadband probe. Chemical shifts (expressed in parts per million) are referenced to the residual solvent peaks.[66] NMR spectra were assigned with the assistance of ^1H-^{13}C (*gs*-HSQC and *gs*-HMBC) correlation experiments.[67] NMR signals due to secondary isomeric forms (where it is possible to assign them) are italicized. Elemental analyses were performed on a Vario MICRO cube instrument (Elementar).

Synthesis of [Ru$_2$Cp$_2$Cl(CO)(μ-CO){μ-η^1:η^2-C(Ph)=CH(Ph)}], 2 (Figure 5).

Figure 5. Structure of **2**.

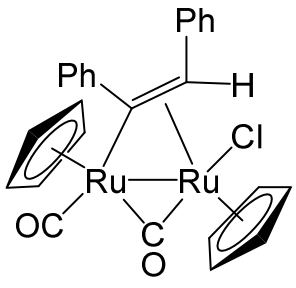

Complex **[1]BF$_4$** (150 mg, 0.220 mmol) was dissolved in CH_2Cl_2 (30 mL) and this solution was treated with a solution of Me_3NO (1.0 eq.) in MeCN (0.10 M). The mixture was stirred for 15 minutes, and the formation of [**1-NCMe**]BF_4 was checked by IR spectroscopy [IR (CH_2Cl_2): $\tilde{\upsilon}/cm^{-1}$ = 1999vs (CO), 1848s (μ-CO)]. Volatiles were removed under vacuum to give an orange residue, which was

dissolved in THF (30 mL), then lithium chloride (105 mg, 2.48 mmol) was added to this solution. The resulting mixture was stirred for 3 hours at room temperature, then the volatiles were removed under reduced pressure. The residue was charged on an alumina column as Et_2O/CH_2Cl_2 (5:1 v/v) solution. Elution with CH_2Cl_2 allowed to separate impurities, then the fraction corresponding to the title compound was eluted using neat THF. The solvent was removed under reduced pressure and the residue was suspended in hexane (50 mL) for 2 h. A red powder was recovered by filtration and dried under vacuum. Yield 92 mg (69%). Anal. calcd. for $C_{26}H_{21}ClO_2Ru_2$: C, 51.66; H, 3.50. Found: C, 51.50; H, 3.54. IR (CH_2Cl_2): $\tilde{\upsilon}/cm^{-1}$ = 1977vs (CO), 1828s (μ-CO). ^1H NMR ($CDCl_3$): δ/ppm = 7.29, 7.18, 7.09, 6.99 (m, 10 H, Ph); 5.34, 4.82 (s, 10 H, Cp); 5.14 (s, 1 H, =CH). $^{13}C\{^1H\}$ NMR ($CDCl_3$): δ/ppm = 229.0, 198.7 (CO); 176.6 (ipso-Ph); 155.1 (Ru-C); 144.6 (ipso-Ph); 128.7, 128.4, 128.4, 127.8, 126.5, 125.9 (Ph); 92.5, 91.0 (Cp); 83.7 (=CH). Crystals of **2** suitable for X-ray analysis were collected by slow diffusion of pentane into a dichloromethane solution of the complex at –30°C.

Synthesis and characterization of complexes [3-7]$^+$.

General procedure. A solution of $[Ru_2Cp_2Cl(CO)_2\{\mu\text{-}\eta^1\text{:}\eta^2\text{-}C(Ph)CH(Ph)\}]$ (**2**, ca. 0.06 mmol) in CH_2Cl_2 (25 mL) was treated with silver salt (1.1 eq.) and with the selected alkyne (> 5 eq.). The reaction mixture was stirred at room temperature in the dark, and the consumption of **2** was checked by IR spectroscopy. Then, the mixture was filtered over a celite pad and volatiles were evaporated from the filtrated solution under reduced pressure. The obtained residue was washed with Et_2O (3 x 20 mL) and finally dried under vacuum.

$[Ru_2Cp_2(CO)_2\{\mu\text{-}\eta^3\text{:}\eta^2\text{-}C(Ph)CH(Ph)C(CO_2Me)C(CO_2Me)\}]CF_3SO_3$, $[3]CF_3SO_3$ (Figure 6).

Figure 6. Structure of [**3**]$^+$.

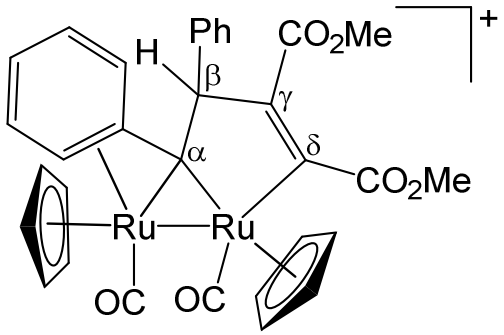

From **2** (30 mg, 0.050 mmol), $AgCF_3SO_3$ (13 mg, 0.051 mmol) and dimethyl acetylenedicarboxylate (0.050 mL, 0.42 mmol). Reaction time: 1h. Brown solid. Yield 22 mg (51%). Anal. calcd. for $C_{33}H_{27}F_3O_9Ru_2S$: C, 46.05; H, 3.16; S, 3.72. Found: C, 45.92; H, 3.23; S, 3.66. IR (CH_2Cl_2): ῡ/cm^{-1} = 2026vs (CO), 2002m (CO), 1712s (CO_2Me). ^1H NMR (acetone-d_6): δ/ppm = 8.32, 7.74, 7.55-7.49, 7.31, 7.21, 7.07-7.03 (m, 10 H, Ph); 6.26 (s, 1 H, $C^{\beta}H$); 5.77, 5.36 (s, 10 H, Cp); 3.80, 3.58 (s, 6 H, Me). $^{13}C\{^1H\}$ NMR (acetone-d_6): δ/ppm = 216.2, 203.0 (CO); 174.8 (C^{α}); 163.5, 161.4 (OCO); 145.5, 142.8 (ipso-Ph); 134.2, 133.4, 130.8, 129.4, 129.4, 128.0 (Ph); 126.2 (C^{δ}); 105.0 (C^{γ}); 93.8, 93.7 (Cp); 74.2 (C^{β}); 51.7, 51.6 (Me). Crystals of **[3]CF_3SO_3** suitable for X-ray analysis were collected by slow diffusion of diethyl ether into a dichloromethane solution of the complex at room temperature.

$[Ru_2Cp_2(CO)_2\{\mu\text{-}\eta^1\text{:}\eta^4\text{-}CHCHC(Ph)CH(Ph)\}]BF_4$, [4]$BF_4$ (Figure 7).

Figure 7. Structure of $[\mathbf{4}]^+$.

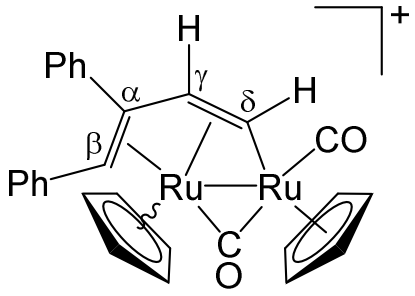

From **2** (30 mg, 0.050 mmol), $AgBF_4$ (11 mg, 0.060 mmol) and acetylene (not quantified large excess) bubbled into the solution. Reaction time: 4 h. Yellow solid. Yield 17 mg (49%). Anal. calcd. for $C_{28}H_{23}BF_4O_2Ru_2$: C, 49.27; H, 3.40. Found: C, 49.15; H, 3.36. IR (CH_2Cl_2): ῡ/cm^{-1} = 2007vs (CO),

1859s (μ-CO). ^{1}H NMR (acetone-d_6): δ/ppm = 11.61, *10.86* (d, $^{3}J_{HH}$ = 8.1 Hz, 1 H, C$^{\delta}$H); *7.60*, 7.49-7.43, 7.25-7.19, 7.02, 6.95 (m, 10 H, Ph); 7.38, *6.80* (d, $^{3}J_{HH}$ = 7.8 Hz, 1 H, C$^{\gamma}$H); 6.22, *5.68*, *5.59*, 5.48 (s, 10 H, Cp); *2.13*, 1.37 (s, 1 H, C$^{\beta}$H). ^{13}C{^{1}H} NMR (acetone-d_6): δ/ppm = *226.0*, 223.5 (μ-CO); 199.1, *194.0* (CO); *166.9*, 165.2 (C$^{\delta}$); 158.6, 138.6 (ipso-Ph); 131.8, 130.9, *130.6*, *130.2*, 129.8, 129.6, 129.1, *128.5*, *127.8*, *127.2* (Ph); 109.9 (C$^{\alpha}$); 99.6, *99.1* (C$^{\gamma}$); *96.8*, 95.2, 90.8, *90.6* (Cp); *86.0*, 80.9 (C$^{\beta}$). Isomer ratio (cis/trans) = 3.3.

[$Ru_2Cp_2(CO)_2${μ-η^1:η^4-C(Me)C(Me)C(Ph)CH(Ph)}]CF_3SO_3, [5]CF_3SO_3 (Figure 8).

Figure 8. Structure of [**5**]$^{+}$.

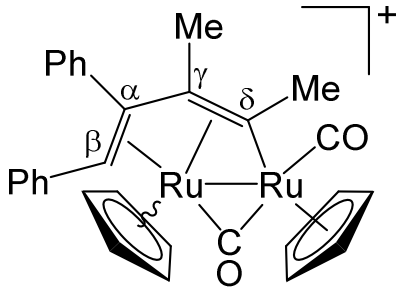

From **2** (33 mg, 0.055 mmol), $AgCF_3SO_3$ (15 mg, 0.060 mmol) and 2-butyne (0.10 mL, 1.3 mmol). Rection time: 12 h. Brown solid. Yield 24 mg (56%). Anal. calcd. for $C_{31}H_{27}F_3O_5Ru_2S$: C, 48.19; H, 3.52; S, 4.15. Found: C, 48.05; H, 3.61; S, 4.12. IR (CH_2Cl_2): ῡ/cm^{-1} = 2008vs (CO), 1884s (μ-CO). ^{1}H NMR (acetone-d_6): δ/ppm = 7.55, *7.46*, 7.42, *7.19*, 7.14-7.05, 6.88 (m, 10 H, Ph); *6.22*, 5.84, *5.61*, 5.41 (s, 10 H, Cp); 3.67, *3.66*, 2.44, *2.35* (s, 6 H, Me); 2.76, *2.60* (s, 1 H, C$^{\beta}$H). ^{13}C{^{1}H} NMR (acetone-d_6): δ/ppm = 219.1 (μ-CO); 195.5 (CO); 180.9 (C$^{\delta}$); 140.4, 138.9 (ipso-Ph); 133.7, 132.9, 130.9, 129.8, 129.4, 129.1, 128.8, 127.7 (Ph); 119.4 (C$^{\alpha}$); 111.9 (C$^{\gamma}$); 93.8, 91.6 (Cp); 74.4 (C$^{\beta}$); 47.2, 23.5 (Me). Isomer ratio (trans/cis) = 5.

[$Ru_2Cp_2(CO)_2${μ-η^1:η^4-C(Ph)C(Ph)C(Ph)CH(Ph)}]CF_3SO_3, [6]CF_3SO_3 (Figure 9).

Figure 9. Structure of [**6**]$^{+}$.

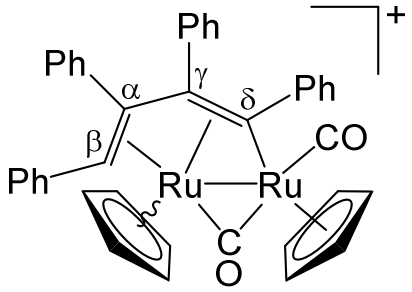

From **2** (35 mg, 0.058 mmol), $AgCF_3SO_3$ (15 mg, 0.060 mmol) and diphenylacetylene (178 mg, 0.999 mmol). Rection time: 12 h. Orange solid. Yield 18 mg (42%). Anal. calcd. for $C_{41}H_{31}F_3O_5Ru_2S$: C, 54.91; H, 3.49; S, 3.57. Found: C, 55.03; H, 3.42; S, 3.62. IR (CH_2Cl_2): $\tilde{\upsilon}/cm^{-1}$ = 2006vs (CO), 1867s (μ-CO). ^1H NMR (acetone-d_6): δ/ppm = 7.37, 7.17, 6.98-6.92, 6.89-6.77, 6.69 (m, 20 H, Ph); 6.00, *5.81*, *5.76*, 5.65 (s, 10 H, Cp); *3.45*, 1.68 (s, 1 H, $C^{\beta}H$). $^{13}C\{^1H\}$ NMR (acetone-d_6): δ/ppm = 220.9 (μ-CO); 199.6 (CO); 188.4 (C^{δ}); 157.8, 138.4, 138.3, 138.1 (ipso-Ph); 134.7-125.4 (Ph); 121.0 (C^{α}); 107.7 (C^{γ}); 97.8, *96.0*, 91.7, *91.5* (Cp); 87.8 (C^{β}). Isomer ratio (cis/trans) = 5.

We failed to collect X-ray quality crystals of **[6]CF_3SO_3**; thus, we performed the synthesis of **[6]BF_4** from **2** and $AgBF_4$, similarly to what described for **[6]CF_3SO_3** (33% yield). The spectroscopic characterization of **[6]BF_4** is reported in the Supporting Information. Then, crystals of **[6]BF_4** suitable for X-ray analysis were collected by slow diffusion of diethyl ether into a dichloromethane solution of the complex at room temperature.

$[Ru_2Cp_2(CO)_2\{\mu\text{-}\eta^1\text{:}\eta^4\text{-}C(Ph)C(H)C(Ph)CH(Ph)\}]CF_3SO_3$, [7]$CF_3SO_3$. (Figure 10).

Figure 10. Structure of [**7**]$^{+}$.

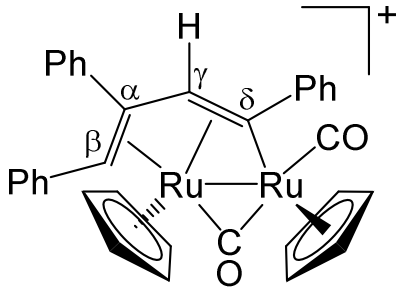

From **2** (35 mg, 0.058 mmol), $AgCF_3SO_3$ (16 mg, 0.064 mmol) and phenylacetylene (0.1 mL, 0.911 mmol). Reaction time: 12h. Brown solid. Yield 20 mg (42%). Anal. calcd. for $C_{35}H_{27}F_3O_5Ru_2S$: C, 51.22; H, 3.32; S, 3.90. Found: C, 51.12; H, 3.35; S, 3.80. IR (CH_2Cl_2): $\tilde{\upsilon}/cm^{-1}$ = 2006vs (CO), 1860s (μ-CO). ^1H NMR (acetone-d_6): δ/ppm = 7.48-7.43, 7.37, 7.34-7.29, 7.10-7.07 (m, 15 H, Ph); 6.80 (s, 1 H, $C^{\gamma}H$); 5.76, 5.74 (s, 10 H, Cp); 1.66 (s, 1 H, $C^{\beta}H$). $^{13}C\{^1H\}$ NMR (acetone-d_6): δ/ppm = 223.0 (μ-CO); 199.0 (CO); 192.6 (C^{δ}); 158.9, 138.6, 137.7 (ipso-Ph); 132.0-125.7 (Ph); 106.9 (C^{α}); 103.3 (C^{γ}); 97.1, *95.0*, *92.3*, 92.1 (Cp); 83.8 (C^{β}).

X-ray crystallography

Crystal data and collection details for **2**, [**3**]$CF_3SO_3 \cdot CH_2Cl_2$ and [**6**]BF_4 are reported in Table 4. Data were recorded on a Bruker APEX II diffractometer equipped with a PHOTON2 detector using Mo–Kα radiation. The structures were solved by direct methods and refined by full-matrix least-squares based on all data using F2.[68] Hydrogen atoms were fixed at calculated positions and refined using a riding model.

Table 4. Crystal data and measurement details for **2**, [**3**]$CF_3SO_3 \cdot CH_2Cl_2$ and [**6**]BF_4.

	2	[**3**]$CF_3SO_3 \cdot CH_2Cl_2$	[**6**]BF_4
Formula	$C_{26}H_{21}ClO_2Ru_2$	$C_{34}H_{29}Cl_2F_3O_9Ru_2S$	$C_{40}H_{31}BF_4O_2Ru_2$
FW	603.02	943.67	832.60
T, K	100(2)	100(2)	100(2)
λ, Å	0.71073	0.71073	0.71073
Crystal system	Monoclinic	Triclinic	Monoclinic
Space group	$P2_1/n$	$P\bar{1}$	$C2/c$
a, Å	9.4345(4)	8.3190(7)	27.3698(8)
b, Å	14.0906(5)	13.7514(12)	18.0419(5)
c, Å	16.9952(6)	15.7743(13)	16.5162(5)
α,°	90	86.749(3)	90
β,°	104.7350(10)	77.108(3)	124.7910(10)
		81.442(3)	90
Cell Volume, Å^3	2185.00(14)	1739.0(3)	6697.8(3)
Z	4	2	8
D_c, g·cm^{-3}	1.823	1.802	1.651
μ, mm^{-1}	1.526	1.153	0.960

F(000)	1192	940	3328
Crystal size, mm	0.24×0.20×0.16	0.16×0.13×0.09	0.18×0.14×0.13
θ limits,°	1.904-26.999	1.975-25.098	1.672-26.999
Reflections collected	32458	19181	50921
Independent reflections	4749 [R_{int} = 0.0261]	6136 [R_{int} = 0.0452]	7307 [R_{int} = 0.0538]
Data / restraints /parameters	4749 / 30 / 280	6136 / 119 / 490	7307 / 0 / 442
Goodness on fit on F^2	1.173	1.137	1.061
R_1 ($I > 2\sigma(I)$)	0.0201	0.0459	0.0345
wR_2 (all data)	0.0456	0.1049	0.0901
Largest diff. peak and hole, e Å^{-3}	0.599 / –0.763	1.195 / –0.882	1.545 / –0.484

DFT calculations

Geometry optimizations were performed using the PBEh-3c method, which is a reparametrized version of PBE0 [69] (with 42 % HF exchange) that uses a split-valence double-zeta basis set (def2-mSVP) with relativistic ECPs for Ru [70,71,72] and adds three corrections that consider dispersion, basis set superposition and other basis set incompleteness effects.[73,74,75] The C-PCM implicit solvation model was added to PBEh-3c calculations, considering dichloromethane as continuous medium.[76,77] Further ground- and transition-state geometry optimizations for selected complexes were carried out by using the hybrid-GGA EDF2 functional[78] in combination with the 6-31G(d,p)/LANL2DZ basis set.[79,80] The localization of the transition states was confirmed by investigating the unique imaginary frequency in the simulated IR spectra and by IRC calculations.[63] All the IR simulations were carried out using the harmonic approximation, from which zero-point vibrational energies and thermal corrections (T = 298.15 K) were obtained. The software used for PBEh-3c calculations was ORCA version 5.0.3,[81] while EDF2 calculations were performed with Spartan‘16 (Wavefunction Inc.), build 2.0.3.[82,83]

Acknowledgements

We thank the University of Pisa for financial support (Fondi di Ateneo 2021).

Supporting Information Available

NMR spectra of products; spectroscopic data of [**6b**]CF_3SO_3; DFT geometries. CCDC reference numbers 2184393 (**2**), 2184394 ([**3**]CF_3SO_3) and 2184395 ([**6**]BF_4) contain the supplementary crystallographic data for the X-ray studies reported in this work. These data are available free of charge at http://www.ccdc.cam.ac.uk/structures.

The authors declare no competing financial interests.

References

1 Desnoyer, A. N.; Nicolay, A.; Rios, P.; Ziegler, M. S.; Don Tilley, T. Bimetallics in a Nutshell: Complexes Supported by Chelating Naphthyridine-Based Ligands, Acc. Chem. Res. 2020, 53, 1944-1956.

2 Deolka, S.; Rivada-Wheelaghan, O.; Aristizabal, S. L.; Fayzullin, R. R.; Pal, S.; Nozaki, K.; Khaskin, E.; Khusnutdinova, J. R. Metal – metal cooperative bond activation by heterobimetallic alkyl, aryl, and acetylide Pt^{II}/Cu^{I} complexes, Chem. Sci., 2020, 11, 5494–5502.

3 Huang, G.-H.; Li, J.-M.; Huang, J.-J.; Lin, J.-D.; Chuang, G. J. Cooperative Effect of Two Metals: $CoPd(OAc)_4$ -Catalyzed C-H Amination and Aziridination, Chem. Eur. J. 2014, 20, 5240 – 5243.

4 Ritleng, V.; Chetcuti, M. J. Hydrocarbyl Ligand Transformations on Heterobimetallic Complexes, Chem. Rev. 2007, 107, 797−858.

5 Tsurugi, H.; Laskar, P.; Yamamoto, K.; Mashima, K. Bonding and structural features of metal-metal bonded homo- and hetero-dinuclear complexes supported by unsaturated hydrocarbon ligands, J. Organomet. Chem. 2018, 869, 251-263.

6 Pétillon, F. Y.; Schollhammer, P.; Talarmin, J. Recent advances in the chemistry of tris(thiolato) bridged cyclopentadienyl dimolybdenum complexes, Coord. Chem. Rev. 2017, 331, 73–92.

7 Knorr, M.; Jourdain, I. Activation of alkynes by diphosphine- and m-phosphido-spanned heterobimetallic complexes, Coord. Chem. Rev. 2017, 350, 217–247.

8 García, M. E.; García-Vivó, D.; Ramos, A.; Ruiz, M. A.; Phosphinidene-bridged binuclear complexes, Coord. Chem. Rev. 2017, 330, 1–36.

9 Mazzoni, R.; Salmi, M.; Zanotti, V. C-C Bond Formation in Diiron Complexes. Chem. Eur. J. 2012, 18, 10174-10194.

10 Biancalana, L.; Marchetti, F. Aminocarbyne ligands in organometallic chemistry. Coord. Chem. Rev. 2021, 449, 214203.

11 Hashimoto, H.; Kurashima, K.; Tobita, H.; Ogino, H. Reactions of a phosphido-bridged unsymmetrical diiron complex $(Cp^*)Fe_2(CO)_4(\mu\text{-}CO)(\mu\text{-}PPh_2)$ with various alkynes, J. Organomet. Chem. 2004, 689, 1481–1495.

12 Dyke, A. F.; Knox, S. A. R.; Naish, P. J.; Taylor, G. E. Organic chemistry of dinuclear metal centres. Part 1. Combination of alkynes with carbon monoxide at di-iron and diruthenium centres: crystal structure of $[Ru_2(CO)(\mu\text{-}CO)\{\mu\text{-}\sigma\text{:}\eta^3\text{-}C(O)C_2Ph_2\}(C_5H_5)_2]$. J. Chem. Soc. Dalton Trans. 1982, 1297-1307.

13 Albano, V. G.; Busetto, L.; Marchetti, F.; Monari, M.; Zacchini, S.; Zanotti, V. Alkyne - Isocyanide Coupling in $[Fe_2(CNMe)(CO)_3(Cp)_2]$: A New Route to Diiron μ-Vinyliminium Complexes, Organometallics 2007, 26, 3448 – 3455.

14 Marchetti, F.; Zacchini, S.; Zanotti, V. Photochemical Alkyne Insertions into the Iron − Thiocarbonyl Bond of $[Fe_2(CS)(CO)_3(Cp)_2]$, Organometallics 2016, 35, 2630−2637.

15 Marchetti, F. Constructing Organometallic Architectures from Aminoalkylidyne Diiron Complexes. Eur. J. Inorg. Chem. 2018, 3987-4003.

16 Rocco, D.; Batchelor, L. K.; Agonigi, G.; Braccini, S.; Chiellini, F.; Schoch, S.; Biver, T.; Funaioli, T.; Zacchini, S.; Biancalana, L.; Ruggeri, M.; Pampaloni, G.; Dyson, P. K.; Marchetti, F. Anticancer Potential of Diiron Vinyliminium Complexes, Chem. Eur. J. 2019, 25, 14801-14816.

17 Wigginton, J. R.; Chokshi, A.; Graham, T. W.; McDonald, R.; Ferguson, M. J.; Cowie, M. Alkyne/Methylene Coupling Reactions at Adjacent Rh/Os Centers: Stepwise Transformations from C_1- through C_4-Bridged Species, Organometallics 2005, 24, 6398 – 6410.

18 Dyke, A. F.; Knox, S. A. R.; Naish, P. J.; Taylor, G. E. Combination of alkynes with m-carbenes at a dimetal centre, and X-Ray structure of $[Fe_2(CO)_2\{\mu\text{-}\eta^1,\eta^3\text{-}C(CO_2Me)C(CO_2Me)CHMe)(Cp)_2]$: implications for metathesis and alkyne polymerisation, J. Chem. Soc. Chem. Commun. 1980, 803-804.

19 Casey, C. P.; Miles, W. H.; Fagan, P. J.; Haller, K. J. Photochemical reaction of μ-ethenylidene complex $[(Cp)(CO)Fe]_2(\mu\text{-}CO)(\mu\text{-}C{=}CH_2)$ with acetylenes, Organometallics 1985, 4, 559-563.

20 A. De Palo, S. Zacchini, G. Pampaloni, F. Marchetti, Construction of a Functionalized Selenophene-Allylidene Ligand via Alkyne Double Action at a Diiron Complex, Eur. J. Inorg. Chem. 2020, 3268–3276.

21 Casey, C. P.; Woo, L. K.; Fagan, P. J.; Palermo, R. E.; Adams, B. R. Reactions of Acetylenes with the Cationic Bridging Methylidyne Complex $[(C_5H_5)(CO)Fe]_2(\mu\text{-}CO)(\mu\text{-}CH)^+$, Organometallics 1987, 6, 447-454.

22 Ciancaleoni, G.; Zacchini, S.; Zanotti, V.; Marchetti, F. DFT Mechanistic Insights into the Alkyne Insertion Reaction Affording Diiron μ-Vinyliminium Complexes and New Functionalization Pathways, Organometallics 2018, 37, 3718−3731.

23 Luh, T.-Y. Trimethylamine N-Oxide-A Versatile Reagent For Organometallic Chemistry. Coord. Chem. Rev. 1984, 60, 255-276.

24 Alvarez, M. A.; García, M. E.; García-Vivó, D.; Huergo, E.; Ruiz, M. A. Acetonitrile Adduct $[MoReCp(\mu\text{-}H)(\mu\text{-}PCy_2)(CO)_5(NCMe)]$: A Surrogate of an Unsaturated Heterometallic Hydride Complex, Inorg. Chem. 2018, 57, 912−915.

25 Boni, A.; Marchetti, F.; Pampaloni, G.; Zacchini, S. Cationic Diiron and Diruthenium l-Allenyl Complexes: Synthesis, X-Ray Structures and Cyclization Reactions with Ethyldiazoacetate/Amine Affording Unprecedented Butenolide- and Furaniminium-Substituted Bridging Carbene Ligands, Dalton Trans., 2010, 39, 10866–10875.

26 de Bruin, B.; Verhagen, J. A. W.; Schouten, C. H. J.; Gal, A. W.; Feichtinger, D.; Plattner, D. A. Enhanced Reactivity of 2-Rhodaoxetanes through a Labile Acetonitrile Ligand, Chem. Eur. J. 2001, 7, 416-422.

27 Ohata, J.; Teramoto, A.; Fujita, H.; Takemoto, S.; Matsuzaka, H. Linear Hydrocarbon Chain Growth from a Molecular Diruthenium Carbide Platform. J. Am. Chem. Soc. 2021, 143, 16105 – 16112, and references therein.

28 Casey, C. P.; Meszaros, M. W.; Fagan, P. J.; Bly, R. K.; Marder, S. R.; Austi, E. A. Hydrocarbation—Formation of Diiron μ-Alkylidyne Complexes from the Addition of the Carbon-Hydrogen Bond of a μ-Methylidyne Complex across Alkenes, J. Am. Chem. Soc. 1986, 108, 4043-4053.

29 Casey, C. P.; Gohdes, M. A.; Meszaros, M. W. Reactions of a Cationic Bridging Methylidyne Complex with Activated Alkenes, Organometallics 1986, 5, 196-199.

30 Boni, A.; Funaioli, T.; Marchetti, F.; Pampaloni, G.; Pinzino, C.; Zacchini, S. Reversible Reductive Dimerization of Diiron μ-Vinyl Complex via C-C Coupling: Characterization and Reactivity of the Intermediate Radical Species, Organometallics 2011, 30, 4115 – 4122.

31 Xing, Y.-K.; Chen, X.-R.; Yang, Q.-L.; Zhang, S.-Q.; Guo, H.-M.; Hong, X.; Mei, T. S. Divergent rhodium-catalyzed electrochemical vinylic C-H annulation of acrylamides with alkynes, Nat. Commun. 2021, 12, 930.

32 Takahashi, T.; Kondakov, D. Y.; Xi, Z.; Suzuki, N. A Vinylzirconation Reaction of Alkynes, J. Am. Chem. Soc. 1995, 117, 5871-5872.

33 Toyofuku, M.; Fujiwara, S.; Shin-ike, T.; Kuniyasu, H.; Kambe, N. Platinum-Catalyzed Intramolecular Vinylchalcogenation of Alkynes with b-Phenylchalcogeno Conjugated Amides, J. Am. Chem. Soc. 2008, 130, 10504–10505.

34 Okauchi, T.; Urakawa, A.; Tabuchi, N.; Arai, M.; Nakagawa, T.; Ichimura, T.; Shimooka, H.; Kitamura, M. Pyrrole Formation via Reactivity of η4-(Vinylketenimine)iron Complexes with Electron-Deficient Alkynes, Organometallics 2021, 40, 2929 – 2933.

35 Trotus, I. T.; Zimmermann, T.; Duyckaerts, N.; Geboers, J.; Schuth, F. Butadiene from acetylene–ethylene cross-metathesis, Chem. Commun., 2015, 51, 7124-7127.

36 Xie, M.; Wang, S.; Wang, J.; Fang, K.; Liu, C.; Zha, C.; Jia, J. Construction of Substituted Benzenes via Pd-Catalyzed Cross-Coupling/Cyclization Reaction of Vinyl Halides and Terminal Alkynes, J. Org. Chem. 2016, 81, 3329−3334.

37 Hofmann, P. The Mechanism of the Dötz Reaction: Chromacyclobutenes by Alkyne–Carbene Coupling? Angew. Chem. Int. Ed. 1989, 28, 908-910.

38 Canovese, L.; Visentin, F.; Chessa, G.; Uguagliati, P.; Santo, C.; Dolmella, A. Insertion of Substituted Alkynes into the Pd - C Bond of Methyl and Vinyl Palladium(II) Complexes Bearing Pyridylthioethers as Ancillary Ligands. The Influence of Ligand Substituents at Pyridine and Sulfur on the Rate of Insertion, Organometallics 2005, 24, 3297-3308.

39 Tomar, V.; Sharma, C.; Nemiwal, M.; Joshi, R. K. Synthesis of novel ferrocenated enynes via the Sonogashira coupling of ferrocenated vinyllic chlorides and alkyne in the catalytic presence of selenated NHC-Pd(II) full pincer complex under Cu and amine free aerobic conditions, J. Organomet. Chem. 2021, 956, 122095.

40 Doherty, N. M.; Howard, J. A. K.; Knox, S. A. R.; Terrill, N. J.; Yates, M. I., Reactivity of Alkenes at a Diruthenium Centre: Combination with Methylene and Oxidative Activation, J. Chem. Soc. Chem. Commun. 1989, 638-640.

41 Dyke, A. F.; Knox, S. A. R.; Morris, M. J.; Naish, P. J. Organic chemistry of dinuclear metal centres. Part 3. μ-Carbene complexes of iron and ruthenium from alkynes via μ-vinyl cations, J. Chem. Soc., Dalton Trans., 1983, 1417-1426

42 Bresciani, G.; Zacchini, S.; Pampaloni, G.; Marchetti, F. Carbon-Carbon Bond Coupling of Vinyl Molecules with an Allenyl Ligand at a Diruthenium Complex, Organometallics 2022, 41, 1006−1014.

43 M. Akita, R. Hua, S. A. R. Knox, Y. Moro-aka, S. Nakanishi, M. I. Yates, Specific C–C coupling of the labile diruthenium bridging methylene complex, $Cp_2Ru_2(\mu\text{-}CH_2)(CO)_2(MeCN)$, with diazoalkanes leading to alkenyl complexes and alkenes. J. Organomet. Chem. 1998, 569, 71-83.

44 G. Bresciani, S. Zacchini, G. Pampaloni, M. Bortoluzzi, F. Marchetti, η^6-Coordinated ruthenabenzenes from three-component assembly on a diruthenium μ-allenyl scaffold, Dalton Trans., 2022, 51, 8390–8400.

45 C. P. Casey, P. C. Vosejpka, Addition of Carbon Nucleophiles to (π-Alkeny1)diiron Complexes, Organometallics 1988, 7, 934-936.

46 P. Q. Adams, D. L. Davies, A. F. Dyke, S. A. R. Knox, K. A. Mead, P. Woodward, Stereochemical control of alkyne oligomerisation at a diruthenium centre: X-ray structures of $[Ru_2(CO)(\mu\text{-}CO)(\mu\text{-}C_4H_4CMe_2)(\eta\text{-}C_5H_5)_2]$ and $[Ru_2(\mu\text{-}CO)\{\mu\text{-}C_4(CO_2Me)_4CH_2\}(\eta\text{-}C_5H_5)_2]$, J. Chem. Soc., Chem. Commun. 1983, 222-224.

47 R. E. Colborn, D. L. Davies, A. F. Dyke, S. A. R. Knox, K. A. Mead, A. G. Orpen, J. E. Guerchais, J. Toue, Organic chemistry of dinuclear metal centres. Part 12. Synthesis, X-ray crystal structure, and reactivity of the di-μ-alkylidene complex $[Ru_2(CO)_2(\mu\text{-}CHMe)(\mu\text{-}CMe_2)(\eta\text{-}C_5H_5)_2]$: alkylidene linking, J. Chem. Soc., Dalton Trans. 1989, 1799-1812.

48 R. E. Colborn, A. F. Dyke, S. A. R. Knox, K. A. Mead, P. Woodward, Organic chemistry of dinuclear metal centres. Part 4. μ-Carbene and μ-vinyl complexes of ruthenium from allenes. J. Chem. Soc., Dalton Trans. 1983, 2099-2108.

49 T. Tako, N. Obayashi, B. Zhao, K. Akiyoshi, H. Omori, H. Suzuki, Synthesis and Property of Diruthenium Complexes Containing Bridging Cyclic Diene Ligands and the Reaction of Diruthenium Tetrahydrido Complex with Benzene Forming a $\mu\text{-}\eta^2\text{:}\eta^2$-Cyclohexadiene Complex via Partial Hydrogenation on a Ru_2 Center. Organometallics 2011, 30, 5057-5067.

50 Lewandos, G. S.; Doherty, N. M.; Knox, S. A. R.; Macpherson K. A.; Guy Orpen, A. Organic chemistry of dinuclear metal centres—X. Dimerization of allene at a diruthenium centre; X-ray crystal structure of $[Ru_2(CO)_2\{(\mu\text{-}C(Me)CHCH_2CCH_2)\}(\eta\text{-}C_5Me_5)_2]$, Polyhedron 1988, 7, 837-845.

51 J. A. Cabeza, I. del Rio, F. Grepioni, M. Moreno, V. Riera, M. Suarez, Reactivity of $[Ru_2(\mu\text{-}\eta^1\text{:}\eta^1\text{-}NCPh_2)(\mu\text{-}\eta^1\text{:}\eta^2\text{-}PhCCHPh)(CO)_6]$ with Alkynes. Insertion Reactions of Nonactivated Alkynes into Ru−C and Ru−N Bonds. Organometallics 2001, 20, 4190-4197.

52 J. A. Cabeza, I. del Rio, P. Garcia-Alvarez, D. Miguel, Reactivity of Diphenylacetylene with a Basal Edge-Bridged Square-Pyramidal Hexaruthenium Cluster. Characterization of Penta-, Hexa-, and Heptanuclear Alkyne Derivatives. Organometallics 2005, 24, 665-672.

53 J. P. H. Charmant, G. Davies, P. J. King, J. R. Wigginton, E. Sappa, Reactivity of a Triruthenium Acetylide Complex toward Alkynes and the Silica-Mediated Dehydration of Cluster-Bound Alkynols: X-ray Crystal Structures of the Novel Butadienyl Species $[Ru_3(CO)_8\{\mu_3\text{-}\eta^8\text{-}C(Bu^t)CC(Ph)C(H)Ph\}]$ and the Unusual Complex $[Ru_3(CO)_5(\mu\text{-}CO)\{\mu_3\text{-}\eta^5\text{-}CC(Bu^t)\text{-}OC(Ph)2CCH\}\{\mu_3\text{-}\eta^6\text{-}CHC(CPh_2OH)COC(CPh_2)CH\}]$, Organometallics, 2000, 19, 2330-2340.

54 Jeffery, J. C.; Moore, I.; Razay, H.; Stone, F. G. A. Protonation of Tolylidyne Ligands bridging Tungsten-Cobalt and -Platinum Bonds; Reactivity of the Cationic Dimetal m-Carbene Complexes Produced etc., J. Chem. Soc. Chem. Commun. 1981, 1255-1258.

55 C. Werlé, R. Goddard, P. Philipps, C. Farès, A. Fürstner, Structures of Reactive Donor/Acceptor and Donor/Donor Rhodium Carbenes in the Solid State and Their Implications for Catalysis, J. Am. Chem. Soc. 2016, 138, 3797−3805.

56 Fischer, H.; Schmid, J.; Riede, J. p-Benzylidenbis(pentacarbonylwolfram)-Komplexe: Thermolyse und Reaktionen mit Alkinen, J. Organomet. Chem. 1988, 355, 219-230.

57 Tang, Y.; Sun, J.; Chen, J. Unusual reactions of cationic carbyne complexes of manganese andrhenium with $[NMe_4][HFe(CO)_4]$ to form heteronuclear dimetal carbene-bridged complexes, J. Chem. Soc., Dalton Trans. 1998, 931–936.

58 Lohner, P.; Pfeffer, M.; Fischer, J. Enlargement of the scope of the carbon–carbon coupling reactionsbetween Fischer-type metallaalkylidyne and organopalladium compounds, J. Organomet. Chem. 2000, 607, 12–17.

59 Akita, M.; Hua, R.; Nakanishi, S.; Tanaka, M.; Moro-oka, Y. Synthesis and Reactivity of Labile MeCN Adducts of Diruthenium Bis(m-methylene) Species, and C-C Coupling with Alkynes and Diazoalkanes, Organometallics 1997, 16, 5572 – 5584.

60 Bordoni, S.; Busetto, L.; Camiletti, C.; Zanotti, V.; Albano, V. G.; Monari, M.; Prestopino, F. Selective Formation of One or Two C - C Bonds Promoted by Carbanion Addition to $[Fe_2(Cp)_2(CO)_2(\mu\text{-}CO)(\mu\text{-}CSMe)]^+$, Organometallics 1997, 16, 1224 – 1232.

61 Dennett, J. N. L.; Knox, S. A. R.; Charmant, J. P. H.; Gillon, A. L.; Orpen, A. G. Synthesis and reactivity of μ-butadienyl diruthenium cations, Inorg. Chim. Acta 2003, 354, 29-40.

62 V. G. Albano, L. Busetto, F. Marchetti, M. Monari, S. Zacchini, V. Zanotti, Diiron μ-Vinyliminium Complexes from Acetylene Insertion into a Metal - Aminocarbyne Bond, Organometallics 2003, 22, 1326-1331.

63 Fukui, K. The path of chemical reactions - the IRC approach. Acc. Chem. Res. 1981, 14, 363–368

64 X. L. R. Fontaine, G. B. Jacobsen, B. L. Shaw, M. Thornton-Pett, Organo-Platinum-lron Complexes containing One Bridging $Ph_2PCH_2PPh_2$ Ligand. Crystal Structures of $[(OC)_3Fe(\mu\text{-dppm})(\mu\text{-CO})Pt(PPh_3)]$, $[(OC)_3Fe(\mu\text{-dppm})\{C(O)C_2H_2\}Pt(PPh_3)]$ and $[(OC)_3Fe(\mu\text{-dppm})(\mu\text{-CMe=}CH_2)Pt(PPh_3)][BF_4]$.

65 Menges, F. "Spectragryph - optical spectroscopy software", Version 1.2.5, @ 2016-2017, http://www.effemm2.de/spectragryph.

66 Fulmer, G. R.; Miller, A. J. M.; Sherden, N. H.; Gottlieb, H. E.; Nudelman, A.; Stoltz, B. M.; Bercaw, J. E.; Goldberg, K. I. NMR Chemical Shifts of Trace Impurities: Common Laboratory Solvents, Organics, and Gases in Deuterated Solvents Relevant to the Organometallic Chemist. Organometallics 2010, 29, 2176–2179.

67 Willker, W.; Leibfritz, D.; Kerssebaum, R.; Bermel, W. Gradient selection in inverse heteronuclear correlation spectroscopy. Magn. Reson. Chem. 1993, 31, 287-292.

68 Sheldrick, G. M. Crystal structure refinement with SHELXL. Acta Crystallogr. C 2015, 71, 3-8.

69 Grimme, S.; Brandenburg, J. G.; Bannwarth, C.; Hansen, A. A. Consistent structures and interactions by density functional theory with small atomic orbital basis sets, J. Chem. Phys. 2015, 143, 054107.

70 Weigend, F.; Ahlrichs, R. Balanced basis sets of split valence, triple zeta valence and quadruple zeta valence quality for H to Rn: Design and assessment of accuracy, Phys. Chem. Chem. Phys. 2005, 7, 3297–3305.

71 Andrae, D.; Haeussermann, U.; Dolg, M.; Stoll, H.; Preuss, H. Energy-adjusted ab initio pseudopotentials for the second and third row transition elements, Theor. Chim. Acta 1990, 77, 123–141.

72 Weigend, F. Accurate Coulomb-fitting basis sets for H to Rn, Phys. Chem. Chem. Phys. 2006, 8, 1057–1065.

73 Kruse, H.; Grimme, S. A geometrical correction for the inter- and intra-molecular basis set superposition error in Hartree-Fock and density functional theory calculations for large systems, J. Chem. Phys. 2012, 136, 154101.

74 Grimme, S.; Ehrlich, S.; Goerigk, L. Effect of the damping function in dispersion corrected density functional theory, J. Comput. Chem. 2011, 32, 1456–1465.

75 Grimme, S.; Antony, J.; Ehrlich, S.; Krieg, H. A consistent and accurate ab initio parametrization of density functional dispersion correction (DFT-D) for the 94 elements H-Pu, J. Chem. Phys. 2010, 132, 154104.

76 Cossi, M.; Rega, N.; Scalmani, G.; Barone, V. Energies, structures, and electronic properties of molecules in solution with the C-PCM solvation model, J. Comput. Chem. 2003, 24, 669–681

77 Barone, V.; Cossi, M. Quantum Calculation of Molecular Energies and Energy Gradients in Solution by a Conductor Solvent Model, J. Phys. Chem. A 1998, 102, 1995–2001.

78 Lin, C. Y.; George, M. W.; Gill, P. M. W. EDF2: A Density Functional for Predicting Molecular Vibrational Frequencies, Aust. J. Chem. 2004, 57, 365−370.

79 Henre, W. J.; Ditchfield, R.; Pople, J. A. Self—Consistent Molecular Orbital Methods. XII. Further Extensions of Gaussian—Type Basis Sets for Use in Molecular Orbital Studies of Organic Molecules, J. Chem. Phys. 1972, 56, 2257-2261.

80 Cramer, C. J. Essentials of Computational Chemistry, 2nd ed.,Wiley, Chichester, 2004.

81 Neese, F. Software update: The ORCA program system - Version 5.0, WIREs Comput. Mol. Sci. 2022, e1616.

82 Shao, Y.; Gan, Z.; Epifanovsky, E.; Gilbert, A. T. B.; Wormit, M.; Kussmann, J.; Lange, A. W.; Behn, A.; Deng, J.; Feng, X.; Ghosh, D.; Goldey, M.; Horn, P. R.; Jacobson, L. D.; Kaliman, I.; Khaliullin, R. Z.; Kus´, T.; Landau, A.; Liu, J.; Proynov, E. I.; Rhee, Y. M.; Richard, R. M.; Rohrdanz, M. A.; Steele, R. P.; Sundstrom, E. J.; Woodcock III, H. L.; Zimmerman, P. M.; Zuev, D.; Albrecht, B.; Alguire, E.; Austin, B.; Beran, G. J. O.; Bernard, Y. A.; Berquist, E.; Brandhorst, K.; Bravaya, K. B.; Brown, S. T.; Casanova, D.; Chang, C.-M.; Chen, Y.; Chien, S. H.; Closser, K. D.; Crittenden, D. L.; Diedenhofen, M.; DiStasio, Jr., R. A.; Do, H.; Dutoi, A. D.; Edgar, R. G.; Fatehi, S.; Fusti-Molnar, L.; Ghysels, A.; Golubeva-Zadorozhnaya, A.; Gomes, J.; Hanson-Heine, M. W. D.; Harbach, P. H. P.; Hauser, A. W.; Hohenstein, E. G.; Holden, Z. C.; Jagau, T.-C.; Ji, H.; Kaduk, B.; Khistyaev, K.; Kim, J.; Kim, J.; King, R. A.; Klunzinger, P.; Kosenkov, D.; Kowalczyk, T.; Krauter, C. M.; Lao, K. U.; Laurent, A. D.;.

83 Spartan ’16, Build 2.0.3, Wavefunction Inc., Irvine CA, USA, 2016.